Eur. Phys. J. B **69**, 357–361 (2009)
DOI: 10.1140/epjb/e2009-00164-9

THE EUROPEAN PHYSICAL JOURNAL B

Regular Article

Omnidirectional reflection and flat-top transmission in Thue-Morse quasicrystal with single-negative materials

C.P. Yin[1], T.-B. Wang[1], J.-W. Dong[1], Y.H. Chen[2], and H.Z. Wang[1,a]

[1] State Key Laboratory of Optoelectronic Materials and Technologies, Zhongshan(Sun Yat-Sen) University, Guangzhou 510275, P.R. China
[2] School of Physics and Telecommunication Engineering, South China Normal University, Guangzhou 510006, P.R. China

Received 14 February 2009 / Received in final form 30 March 2009
Published online 8 May 2009 –

Abstract. By means of transfer matrix method, we investigate the transmittance and reflectance of Thue-Morse (T-M) structure composed of negative-permittivity and negative-permeability materials. It is shown that the width and location of an omnidirectional reflectance band remain invariant with the change of generation order, and that the omnidirectional reflectance band is determined by both TE and TM polarization, which different completely from that in dielectric T-M structure. Moreover, a flat-top total transmission band occurs around the same frequency in which the general zero average permittivity and permeability are both satisfied in T-M structure. The basis for these phenomena are presented and discussed.

PACS. 42.70.Qs Photonic bandgap materials – 41.20.Jb Electromagnetic wave propagation; radiowave propagation – 71.23.Ft Quasicrystals

1 Introduction

There has been much interest during the last few years in the area of artificially structured materials with unusual electromagnetic properties known as metamaterials [1–5]. There are mainly two kinds of metamaterials: one is the double-negative materials in which permittivity (ε) and permeability (μ) are both negative; the other is the single-negative (SNG) materials, which include the mu-negative (MNG) materials with negative μ but positive ε and the epsilon-negative (ENG) materials with negative ε but positive μ. Owing to the fact that SNG materials support only evanescent waves, unique transmission properties have been reported in structures containing SNG materials. For example, ENG-MNG bilayer structure show a number of properties such as resonance, complete tunneling and transparency [5]; one dimensional photonic crystals consisting of MNG and ENG exhibit a zero effective phase (zero-ϕ_{eff}) gap, which is omnidirectional and insensitive to disorder [6,7]; twin defect modes are found in photonic crystals with SNG materials defect [8,9], and so on.

Quasicrystal is a kind of non-period structure which lacks long-range translational symmetry, but possesses a certain orientation order. The structural ordering of quasicrystal is between the periodic and disordered systems [10,11]. The study of the propagation and the localization of light in one dimensional quasicrystal were largely developed during the last decades [12,16]. Two well-known examples of one dimensional quasicrystal are the Fibonacci and Thue-Morse (T-M) structures. Contrasting with the Cantor-set spectrum and critical eigenstates of the Fibonacci structure, the T-M structure has singular continuous Fourier spectrum and supports the appearance of extended states. Such difference makes the T-M structure showing much more interesting properties. In addition to traditional gap, the dielectric T-M systems may exhibit fractal gap, in case fractal structures are involved [17]. The scaling of the fractal gaps occurring in dielectric T-M multilayer provides a large omnidirectional band gap [18,19].

Recently, the band gaps of Fibonacci photonic crystals with double-negative materials have been presented [20–23]. These studies treated the Fibonacci sequence as a complex basis and observe that the change in the width and location of omnidirectional zero-$\bar{n}$ gap is limited for the Fibonacci photonic crystals with different generation orders [22,23]. In this paper, we introduce the SNG materials into T-M structure to study the reflection and transmission of any order T-M structure rather than treating them as a complex basis. The rest of the paper is organized as follows: in Section 2, we briefly introduce the theoretical model and numerical method. Section 3 gives the reflectance of higher order T-M structures. The results show an omnidirectional reflectance band which determined not only by TE polarization but also by TM

[a] e-mail: stswhz@mail.sysu.edu.cn

polarization exists in higher order T-M structure. In Section 4, we investigate the flat-top transmission band in T-M structures. The conclusions are given in Section 5.

2 Theoretical model and numerical method

The system under consideration is composed of two layers A and B stacked alternatively along z direction and following the rules of T-M sequence, that is, $S_n = S_{n-1}\bar{S}_{n-1}$ with $S_1 = AB$, here n represents the T-M order and $\bar{S}_{n-1}$ is the complement of S_{n-1} obtained by interchanging A and B in S_{n-1}. The lower order T-M sequences are represented by the strings $S_1 = AB$, $S_2 = ABBA$, $S_3 = ABBABAAB$ and so on. The number of layers in this systems increases with n as 2^n, while the ratio of the number of layer A to the number of layer B is equal to unity. In this study, layer A, B represent ENG materials with thickness d_A and MNG materials with thickness d_B respectively. Based on the proposed numerical analysis and experiments for SNG materials [6,7,24], ENG and MNG materials are assumed to isotopic; frequency dependent ε and μ are supposed

$$\varepsilon_A = \varepsilon_a - \frac{\omega_{ep}^2}{\omega^2}, \quad \mu_A = \mu_a \tag{1}$$

in ENG materials and

$$\varepsilon_B = \varepsilon_b, \quad \mu_B = \mu_b - \frac{\omega_{mp}^2}{\omega^2} \tag{2}$$

in MNG materials, where ω is the angular frequency with units of GHz. ω_{ep} and ω_{mp} are, respectively, the electronic and magnetic plasma frequencies. In the following calculation, we choose $\varepsilon_a = \mu_b = 1, \mu_a = \varepsilon_b = 3$, and $\omega_{mp} = \omega_{ep} = 10$ GHz.

Let a transverse electric (TE) wave be incident at an angle θ from vacuum onto the n-th order T-M multilayer. The electric and magnetic component in z and $z + \Delta z$ can be related by a transfer matrix [25]

$$M_i(\Delta z) = \begin{pmatrix} \cosh k_i \Delta z & \frac{\mu_i}{\sqrt{|\varepsilon_i\mu_i|+\sin^2\theta}} \sinh k_i \Delta z \\ \frac{\sqrt{|\varepsilon_i\mu_i|+\sin^2\theta}}{\mu_i} \sinh k_\mu \Delta z & \cosh k_{_i} \Delta z \end{pmatrix} \quad (i = A, B) \tag{3}$$

where $k_i = \frac{\omega}{c}\sqrt{|\varepsilon_i\mu_i| + \sin^2\theta}$, c is the speed of light in vacuum. Suppose the regions outside of the system are vacuum, the reflection and transmission coefficient of monochromatic plane wave are given by:

$$r(\omega) = \frac{(X_{n,22} - X_{n,11})\cos\theta + i(X_{n,12}\cos^2\theta + X_{n,21})}{(X_{n,22} + X_{n,11})\cos\theta + i(X_{n,12}\cos^2\theta - X_{n,21})}, \tag{4}$$

$$t(\omega) = \frac{2\cos\theta}{(X_{n,22} + X_{n,11})\cos\theta + i(X_{n,12}\cos^2\theta - X_{n,21})}. \tag{5}$$

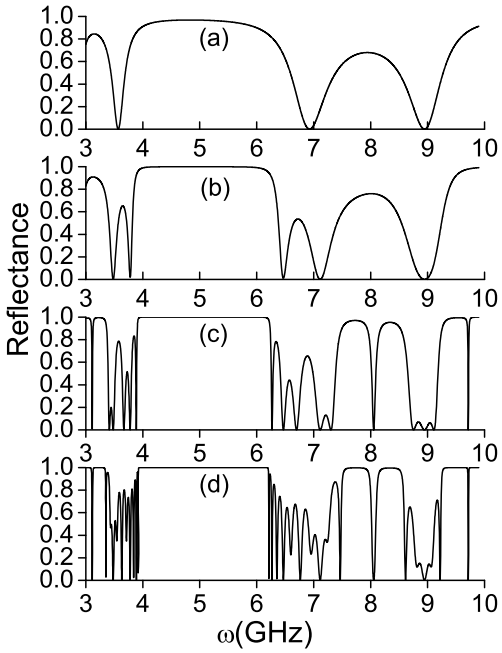

Fig. 1. Normal incidence reflection spectra for the different order T-M structures as a function of the angular frequency (a) S_4; (b) S_5; (c) S_6; (d) S_7.

Here, $X_{n,ij}$ $(i, j = 1, 2)$ are the matrix elements of X_n which is the total transfer matrix of the n-th order T-M sequence. The X_n can be deduced from the following recursion relation:

$$X_n = X_{n-1}\bar{X}_{n-1} \text{ with } X_1 = M_A(d_A)M_B(d_B) \tag{6}$$

where $\bar{X}_{n-1}$ is the complement of X_{n-1} obtained by interchanging A and B in X_{n-1}. The treatment for transverse magnetic (TM) wave is similar to that for TE wave.

3 Omnidirectional reflection in higher order T-M structures

In this section, we choose $d_A = 12$ mm, $d_B = 6$ mm to study the reflection spectra for higher order $(n \geqslant 4)$ T-M quasicrystal. In Figure 1, the reflection spectra for normal incidence are shown in case of S_4 (Fig. 1a), S_5 (Fig. 1b), S_6 (Fig. 1c) and S_7 (Fig. 1d) T-M structures. It can be seen from Figure 1 that, on the increasing the order of T-M structures, a large reflectance band centered at the angular frequency of 5 GHz remains invariant and the edges of band becomes much sharper. Moreover, very narrow transmission peaks appear and split the reflectance band into two parts at higher frequencies. In fact, the reflectance band can be occurred in all higher order T-M structures. For simplicity, others are not given in this paper.

The phenomenon can be explained as follows. In the long-wavelength limit, the multilayer structure behaves as an effective medium whose response is determined by the

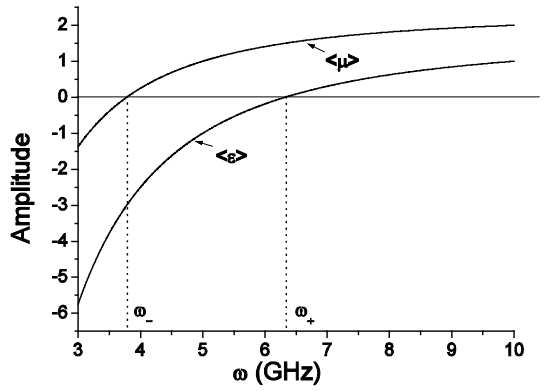

Fig. 2. The curves of the amplitude of average permittivity and average permeability versus the angular frequency with $d_A = 12$ mm and $d_B = 6$ mm.

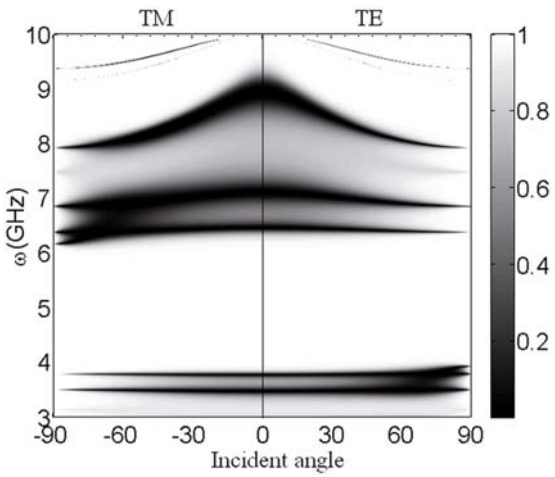

Fig. 3. (Color online) Dependence of TM- and TE-polarization reflection spectra (left and right parts of the plot respectively) for the S_5 T-M structures.

general average ε and μ [23]. For any given order T-M structure, the general average ε and μ can be written as

$$\langle\varepsilon\rangle = \frac{N_A\varepsilon_A d_A + N_B\varepsilon_B d_B}{N_A d_A + N_B d_B}, \tag{7}$$

$$\langle\mu\rangle = \frac{N_A\mu_A d_A + N_B\mu_B d_B}{N_A d_A + N_B d_B}. \tag{8}$$

where N_A, N_B represent the number of ENG and MNG materials in any order T-M structure, respectively. According to the recursion rules of T-M structure, the number of layer A equals to the number of layer B, namely $N_A = N_B$. Then equations (7) and (8) can be simplified as $\langle\varepsilon\rangle = \frac{\varepsilon_A d_A + \varepsilon_B d_B}{d_A + d_B}$, $\langle\mu\rangle = \frac{\mu_A d_A + \mu_B d_B}{d_A + d_B}$, respectively. Figure 2 shows the curves of those averaged values versus the angular frequency. It's shown that when the angular frequency is between ω_-(the zero-point of $\langle\mu\rangle = 0$) and ω_+(the zero point of $\langle\varepsilon\rangle = 0$), $\langle\mu\rangle$ is greater than zero and $\langle\varepsilon\rangle$ is less than zero. So the refractive index of the effective medium is imaginary. Hence, the effective medium does not allow the propagation of the electromagnetic wave, and the corresponding frequency range should be a gap of the structure. Keeping the radio of d_A/d_B constant and increasing the thickness of d_A and d_B simultaneously, ω_- (the root of $\langle\mu\rangle = 0$) and ω_+(the root of $\langle\varepsilon\rangle = 0$) keep invariant. So the gap width is invariant to scaling. Because the number of layer A does not equal to the number of layer B in other kind of quasicrystal, the gap would be changed with the increasing generation order.

It must be noted that the center of large reflectance band in the above is equal to that of zero-ϕ_{eff} gap occurred in photonic crystals constructed by ENG and MNG materials [6]. A natural question to ask is, can the reflectance band in the T-M structures share the same omnidirectional properties as zero-ϕ_{eff} gap? The answer is the affirmative. We take the S_5 as an example and investigate the wide angle reflectance behavior of the systems. In Figure 3, we show reflectance for both TE (the right part) and TM (the left part) polarizations versus angular frequency for different incident angle up to 90°. It's illustrated that the higher band edge of reflection band is insensitive to the increase of the incident angle and the lower band edge shift towards high frequency for TE polarization, but the case for TM polarization is different, the lower band edge nearly keep constant and the higher band edge shift towards low frequency. So the frequency range of the omnidirectional reflectance band for both polarizations is between 4.2 GHz and 5.8 GHZ, which is determined by the higher band edge for TM polarization and the lower band edge for TE polarization. The property is similar to omnidirectional reflection band coming from zero-$\bar{n}$ gap mechanisms in one-dimensional photonic crystals containing anisotropic left-handed materials [26]. But the property is different fundamentally from that of omnidirectional reflection band in dielectric T-M structures [18], in which omnidirectional reflection band depended only on TM polarization. The main reason for different results is because their mechanisms of the band formation are different. The band formation comes from light scattering of propagating modes in dielectric T-M structures; while for T-M structures with SNG materials, it originates from light tunneling of evanescent modes.

4 Flat-top response in T-M structures

In reference [27], it's pointed out that a multilayer structure composed of ENG and MNG materials can be perfectly transparent as long as the general zero average ε and μ are both satisfied. For any order T-M structure, it means that equations (7) and (8) are both equal to zero. If we choose $d_A = d_B$, equations (7) and (8) are both equal to zero at $\omega = 5$ GHz, and then any order T-M structure will become transparent around the frequency point. In Figure 4, we calculate the transmittance of S_2 (Fig. 4a), S_3 (Fig. 4b) and S_4 (Fig. 4c) T-M structures when $d_A = d_B = 20$ mm. It can be seen from the figures that all these structures have total transmission band with flat-top shape which occur around the same frequency $\omega = 5$ GHz. Then these structures become completely

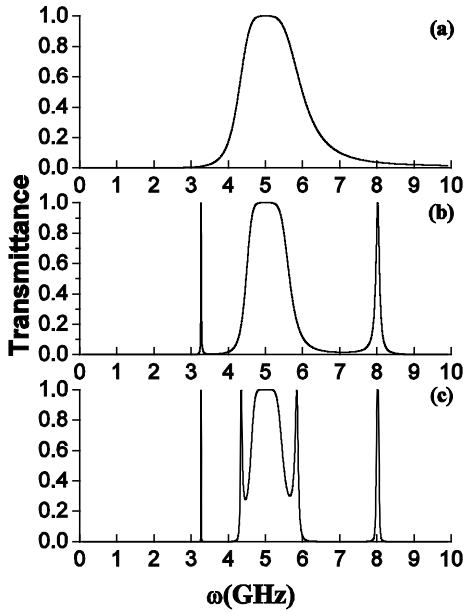

Fig. 4. Linear transmission spectra for plane waves at normal incidence for the lower-order T-M structures with $d_A = d_B =$ 20 mm (a) S_2; (b) S_3; (c) S_4.

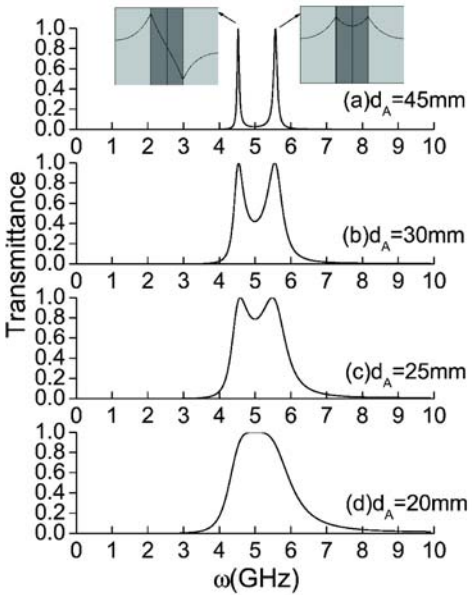

Fig. 5. (Color online) Dependence of normal incidence transmission spectra for the S_2 T-M structures on d_A with $d_B =$ 20 mm (a) $d_A = 45$ mm; (b) $d_A = 30$ mm; (c) $d_A = 25$ mm; (d) $d_A = 20$ mm. The insets plot the electric-field profile corresponding to the tunneling modes.

transparent for electromagnetic wave whose frequency fall within the frequency range.

In order to better understand the physical mechanism of the flat-top total transmission in T-M structures, we study the evolution of transmittance characteristics. Figure 5 shows normal incidence transmission spectra for S_2 T-M structures with the change of d_A (keep $d_B =$ 20 mm constant). From Figure 5a, we can see that, when

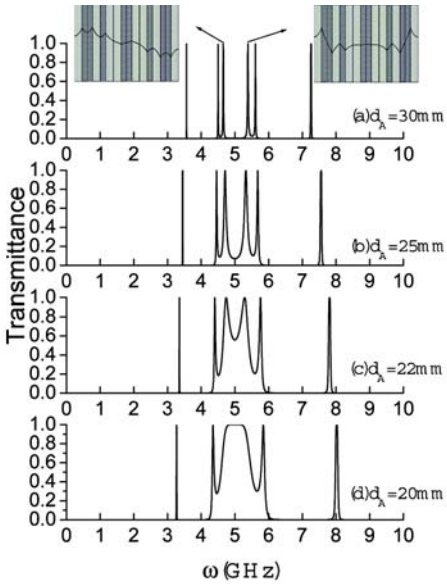

Fig. 6. (Color online) Dependence of normal incidence transmission spectra for the S_4 T-M structures on d_A with $d_B =$ 20 mm (a) $d_A = 30$ mm; (b) $d_A = 25$ mm; (c) $d_A = 22$ mm; (d) $d_A = 20$ mm. The insets plot the electric-field profile corresponding to the tunneling modes.

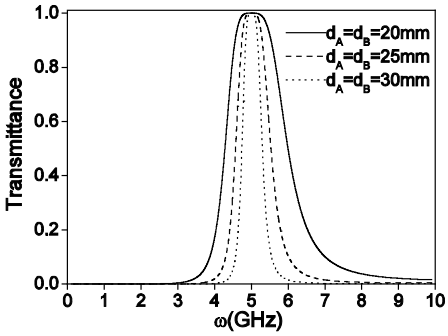

Fig. 7. Normal incidence transmission spectra for the S_2 T-M structure with $d_A = d_B = 20$ mm (solid line), 25 mm (dashed line) and 30 mm (dotted line).

$d_A = 45$ mm, two tunneling modes with unity transmission occur at angular frequency $\omega = 4.525$ GHz and $\omega = 5.568$ GHz. Their electric field distributions show asymmetric and symmetric behavior as depicted in the inset of Figure 5a. We can call them asymmetric and symmetric tunneling modes. As d_A decrease, the two modes gradually draw together until a flat-top transmission band emerges when $d_B = 20$ mm. A similar analysis has been made for S_4 T-M structures. The results are depicted in Figure 6. It's obvious seen from the figure that the formation process of flat-top band in S_4 structures is the same as that in S_2 structures. Therefore it can be concluded that the flat-top transmission band formed by emerging the asymmetric and symmetric tunneling modes.

Next, we turn our attention to the effect of the thickness of ENG and MNG materials on the width of the flat-top total transmission band in S_2 T-M structures. Figure 7 shows that an increase in the thickness of ENG

and MNG materials leads to a decrease in the width of flat-top region. At the same time, the band edges of flat-top transmission band become much steeper. The properties are different from that of omnidirectional reflectance band discussed in the above, which keep invariant when increasing the thickness of ENG and MNG materials simultaneously. Such properties can be used to design band-pass filter with tunable bandwidth.

5 Conclusion

In summary, the transmittance and reflectance of one dimensional quasicrystal structure composed by ENG materials A and MNG materials B, arranged according to recursion rule of the T-M type, have been studied. We have proven that an omnidirectional reflectance band which determined not only by TE polarization but also by TM polarization exists, and that the width and location of the band remain unchanged with the increase of generation order. Moreover, a flat-top total transmission band can be achieved in T-M structure by the merging the symmetric and asymmetric tunneling modes. These results could lead to further applications of the T-M structure.

This work is supported by the National Natural Science Foundation of China (10874250, 10674183, 10804131), National 973 Project of China (2004CB719804), and PhD Degrees Foundation of Education Ministry of China (20060558068).

References

1. J.B. Pendry, Phys. Rev. Lett. **85**, 3966 (2000)
2. D.R. Smith, N. Kroll, Phys. Rev. Lett. **85**, 2933 (2000)
3. R.A. Shelby, D.R. Smith, S. Schultz, Science **292**, 77 (2001)
4. D.R. Fredkin, A. Ron, Appl. Phys. Lett. **81**, 1753 (2002)
5. A. Alù, N. Engheta, IEEE Trans. Antennas Propag. **51**, 2558 (2003)
6. H.T. Jiang, H. Chen, H.Q. Li, Y.W. Zhang, J. Zi, S.Y. Zhu, Phys. Rev. E **69**, 066607 (2004)
7. L.G. Wang, H. Chen, S.Y. Zhu, Phys. Rev. B **70**, 245 (2004)
8. Y.H. Chen, J.W. Dong, H.Z. Wang, Appl. Phys. Lett. **89**, 141101 (2006)
9. Y.H. Chen, Appl. Phys. Lett. **92**, 011925 (2008)
10. *Quasicrystals*, edited by T. Fujiwara, T. Ogawa (Springer, Heidelberg, 1990)
11. M. Kohmoto, B. Southerland, C. Tang, Phys. Rev. B **35**, 1020 (1987)
12. M. Dulea, M. Severin, R. Riklund, Phys. Rev. B **42**, 3680 (1990)
13. W. Gellermann, M. Kohmoto, B. Southerland, P.C. Taylor, Phys. Rev. Lett. **72**, 633 (1994)
14. J.W. Feng, G.J. Jin, A. Hu, S.S. Jiang, D. Feng, Phys. Rev. B **52**, 15312 (1995)
15. N.H. Liu, Phys. Rev. B **55**, 3543 (1997)
16. E.L. Albuquerque, M.G. Cottam, Phys. Rep. **376**, 225 (2003)
17. X. Jiang, Y. Zhang, S. Feng, K.C. Huang, Y. Yi, J.D. Joannopoulos, Appl. Phys. Lett. **86**, 201110 (2005)
18. L.D. Negro, M. Stolfi, Y. Yi, J. Michel, X. Duan, L.C. Kimerling, J. LeBlanc, J. Haavisto, Appl. Phys. Lett. **84**, 5186 (2004)
19. L. Moretti, I. Rea, L. Rotiroti, I. Rendina, G. Abbate, A. Marino, L.De. Stefano, Opt. Express **14**, 6264 (2006)
20. J. Li, D. Zhao, Z. Liu, Phys. Lett. A **332**, 461 (2004)
21. M.S. Vasconcelos, P.W. Mauriz, F.F. de Medeiros, E.L. Albuquerque, Phys. Rev. B **76**, 165117 (2007)
22. W.J. Hsueh, C.T. Chen, C.H. Chen, Phys. Rev. A **78**, 013836 (2008)
23. A. Bruno-Alfonso, E. Reyes-Gómez, S.B. Cavalcanti, L.E. Oliveira, Phys. Rev. A **78**, 035801 (2008)
24. G.V. Eleftheriades, A.K. Iyer, P.C. Kremer, IEEE Trans Microwave Theory Tech. **50**, 2702 (2002)
25. H.T. Jiang, H. Chen, H.Q. Li, Y.W. Zhang, S.Y. Zhu, J. Appl. Phys. **98**, 013101 (2005)
26. S. Wang, L. Gao, Eur. Phys. J. B **48**, 29 (2005)
27. G.S. Guan, H.T. Jiang, H.Q. Li, Y.W. Zhang, H. Chen, S.Y. Zhu, Appl. Phys. Lett. **88**, 211112 (2006)